

Up-current geomorphic events and local tectonics as primary controls on sediment transport by the West Spitsbergen Current and sedimentation in the Fram Strait since ca. 3 Ma

K. St John^{1,*}, R.G. Lucchi², T.A. Ronge³, B. Reilly⁴, J. Gruetzner⁵, Y. Sakai⁶, A.C. Gebhardt⁵, A. Gonzalez-Lanchas⁷, J.E. Johnson⁸, A. Plaza-Faverola⁹, Y. Suganuma¹⁰, M.A. Bárcena¹¹, S. De Schepper¹², L.C. Duxbury¹³, G. Goss¹⁴, N. Greco¹⁵, L. Haygood¹⁶, K. Husum¹⁷, M. Iizuka¹⁸, A.K.I.U. Kapuge¹⁹, A.R. Lam²⁰, O. Libman-Roshal²¹, Y. Liu²², L.R. Monito²³, Y. Rosenthal²⁴, A.V. Sijinkumar²⁵, and Y. Zhong²⁶

¹Department of Geology and Environmental Science, James Madison University, Harrisonburg, Virginia 22807, USA

²Instituto Nazionale di Oceanografia e di Geofisica Sperimentale, 34010 Sgonico (Trieste), Italy

³Scientific Ocean Drilling, Texas A&M University, College Station, Texas 77845, USA

⁴Lamont-Doherty Earth Observatory (LDEO), Columbia University, Palisades, New York 10964, USA

⁵Alfred Wegener Institute Helmholtz Center for Polar and Marine Research, Bremerhaven 27568, Germany

⁶Kyoto University, Graduate School of Engineering, Department of Urban Management, Kyoto-fu 615-8540, Japan

⁷Department of Earth Sciences, University of Oxford, Oxford OX1 3AN, UK

⁸University of New Hampshire, Durham, New Hampshire 03824, USA

⁹Department of Geosciences, The Arctic University of Norway, 9019 Tromsø, Norway

¹⁰National Institute of Polar Research, Tachikawa, Tokyo 190-0014, Japan

¹¹University of Salamanca, 37008 Salamanca, Spain

¹²NORCE Research and Bjerknes Centre for Climate Research, N-5007 Bergen, Norway

¹³Institute for Marine and Antarctic Studies, Battery Point, Tasmania 7004, Australia

¹⁴Department of Earth and Planetary Sciences, Yale University, New Haven, Connecticut 06511, USA

¹⁵National Center for Ecological Analysis and Synthesis (NCEAS), University of California Santa Barbara, Santa Barbara, California 93101, USA

¹⁶Boone Pickens School of Geology, Oklahoma State University, Stillwater, Oklahoma 74075, USA

¹⁷Norwegian Polar Institute, Tromsø NO-9007, Norway

¹⁸National Institute of Advanced Industrial Science and Technology, Marine Geology Research Group, 1-1-1 Higashi, Japan

¹⁹Department of Earth Sciences, University of Delaware, Newark, Delaware 19716, USA

²⁰Earth Sciences, Binghamton University, Binghamton, New York 13902, USA

²¹Earth and Environmental Studies, Montclair State University, Montclair, New Jersey 07043, USA

²²First Institute of Oceanography, Kay Laboratory of Marine Geology and Metallogeny, Qingdao 266061, China

²³Department of Geological Sciences, University of Florida, Gainesville, Florida 32607, USA


²⁴Institute of Marine and Coastal Sciences, Rutgers, The State University of New Jersey, New Brunswick, New Jersey 08901, USA

²⁵Department of Geology, Central University of Kerala, Kerala 671320, India

²⁶Advanced Institute of Ocean Research, Department of Ocean Science and Engineering, Southern University of Science and Technology, Shenzhen 518055, China

ABSTRACT

International Ocean Discovery Program Expedition 403 recovered the longest sediment cores from the Svyatogor Ridge (SR) and Vestnesa Ridge (VR) to date, enabling hypothesis testing of competing influences on sediment drift evolution in the Fram Strait, with implications for ocean circulation. We found that regional geomorphic events and local tectonics

Kristen St John  <https://orcid.org/0000-0001-7045-7485>
*stjohnke@jmu.edu

CITATION: St John, K., et al., 2026, Up-current geomorphic events and local tectonics as primary controls on sediment transport by the West Spitsbergen Current and sedimentation in the Fram Strait since ca. 3 Ma: *Geology*, v. XX, p. , <https://doi.org/10.1130/G54231.1>

exerted first-order controls on Pliocene–Pleistocene accumulation rates in eastern Fram Strait sediment drift through modulation of sediment supply to the West Spitsbergen Current (WSC) and depositional accommodation space. Expedition 403 drill cores show significant reductions in sediment deposition ca. 2 Ma and ca. 1 Ma. Linear sedimentation rates (LSRs) were more than twice as high at SR compared to VR before ca. 2 Ma, suggesting SR was a more significant depocenter than previously thought. This disparity appears to be linked to tectonically influenced paleobathymetry associated with extensional faulting. A major decrease in LSRs ca. 2 Ma coincided with the Barents Shelf changing from subaerial to marine, likely reducing erosion and sediment supply to the WSC. A further decrease in LSRs occurred ca. 1 Ma, during the mid-Pleistocene transition. This change aligns with increased Barents Seaway excavation, suggesting that reduced sediment input to the northern margins relates to a reorganization of ocean circulation. A weakened WSC no longer served as the only route for current flow and sediment transport from the North Atlantic to the Arctic Ocean, as the Barents Sea route was also viable when ice free.

INTRODUCTION

Flowing to the Arctic Ocean through the eastern Fram Strait (FS), the West Spitsbergen Current (WSC) is the northernmost extension of the North Atlantic Current (NAC), and it is the primary source of heat, salt, and moisture to the Arctic region. This influx of warm, salty water is thought to control the extent and dynamics of Arctic ice sheets and sea ice (Kremer et al., 2018), and in turn, past and future global climate variability.

Given the importance of the WSC as a player in the ocean-climate system, International Ocean Discovery Program Expedition 403 (IODP Exp403) drilled several sediment drift sites (Fig. 1) to obtain core records suitable to reconstruct past WSC variability, particularly across global climate transitions. Sediment drifts are mounded depocenters that form under the influence of bottom contour currents (contourites) persistent over millions of years (Rebesco et al., 2014).

Two sediment drifts under the influence of the paleo-WSC are the Vestnesa Ridge (VR)

and the Svyatogor Ridge (SR). The VR is an ~100 km elongate drift extending from the Svalbard continental margin, likely shaped by a westward-turning branch of the WSC. It lies east of the Molloy Ridge (MR) and north of the Molloy Transform Fault (MTF) and overlies the ocean-continent transition (Eiken and Hinz, 1993). The SR is a sediment drift (~45 km long; Johnson et al., 2015; Waghorn et al., 2018) extending off the NW flank of the Knipovich Ridge (KR) at the inner oblique junction with the MTF (Amundsen et al., 2011; Dumais et al., 2021); it overlies very young oceanic crust (ca. 7.3 Ma; Gaina, 2014) and is in an active rift environment with associated detachment faults (Waghorn et al., 2018). Both the MR and KR are ultraslow spreading ridges.

The way in which the tectonic evolution of this complex ridge-transform system has influenced the development of sediment drifts in the region remains poorly understood. Informed by the paleocurrent contourite models of Eiken and Hinz (1993), Amundsen et al. (2011) hypothesized thick sediment packages built up within

active half grabens on the western flank of the KR (i.e., at SR). Johnson et al. (2015) postulated that the VR and the SR were once connected and that a south-to-north bathymetric down-step across the MTF enhanced sediment accumulation north of the fault (i.e., at VR). In their reconstruction, the sediment drift buildup at the SR was thought to be much delayed. It was proposed to have started only when sediment delivery increased with the intensification of the Northern Hemisphere glaciation (iNHG; ca. 2.7 Ma) and the onset of shelf-edge glaciation of the paleo-Svalbard–Barents Sea Ice Sheet. Their observation of ridge-crest displacement suggested that the SR shifted westward over the past 2 m.y., away from a main path of the WSC, resulting in reduced sedimentation since that time.

Farther afield, modeling-based studies (Butt et al., 2002; Zieba et al., 2017; Patton et al., 2024) suggested that large expanses of the Eurasian Arctic switched from subaerial exposure to marine conditions ca. 2 Ma and that the Barents Seaway was open intermittently since 1 Ma and persistently since ca. 0.7 Ma. The latter time interval spans the mid-Pleistocene transition (MPT; Herbert, 2023). Barker et al. (2021) documented increased heat transport to the Nordic Seas via the NAC during the MPT and hypothesized increased Atlantic water inflow to the Arctic Ocean. Given that the NAC transitions to the WSC north of the Barents Seaway, we hypothesized that corroborating evidence for these events should exist in sediment drifts of the Fram Strait. Presumably, erosion rates would affect sediment supply to the WSC, and the diversion of the NAC into the shallow (~450 m) Barents Sea could affect the strength of the WSC heading to the Fram Strait.

In combination, the former hypotheses (Amundsen et al., 2011; Johnson et al., 2015; Barker et al., 2021; Patton et al., 2024) suggest a complex interplay of tectonic influences on local bathymetry and climatic and distant geomorphic influences on sediment input as controlling factors for sedimentation by the paleo-WSC. The hypothesized timing and pattern of depocenter evolution across the MTF can now be tested with the stratigraphic records from the Exp403 SR and VR drill sites. Exp403 recovered the longest sediment core records from these sediment drifts to date (Lucchi et al., 2026), extending hundreds of meters deeper than previous coring. In this study, we used Exp403 shipboard age models, long-term average linear sedimentation rates (LSRs), and lithologies from VR and SR drill sites to document the evolution of the drifts over the past 3 m.y. We then assessed if the proposed tectonic, geomorphic, and paleoceanographic changes in the region impacted sediment input to the main northward-flowing WSC and the strength variation of that current.

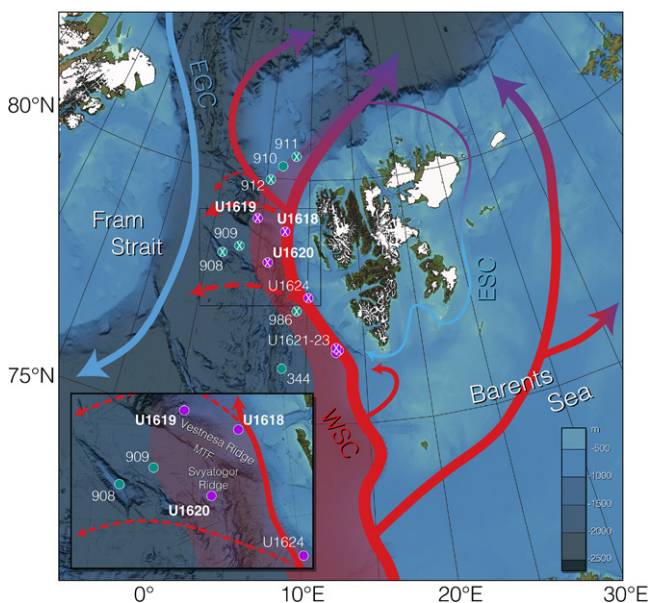


Figure 1. Map of International Ocean Discovery Program Expedition 403 (Exp403) sites (purple) and Ocean Drilling Program (ODP)/Deep Sea Drilling Project (DSDP) sites (teal) in the path of West Spitsbergen Current (WSC; red arrow and swath). Sites with crosses show decreased linear sedimentation rates (LSRs) at ca. 1 Ma. Recirculating current (dashed lines) placement is based on Walczowski and Piechura (2011) and Kalhagen et al. (2024). EGC—East Greenland Current; ESC—East Spitsbergen Current. Inset map: Bathymetric setting of Svyatogor Ridge (SR) and Vestnesa Ridge (VR) sediment drifts. MTF—Molloy transform fault.

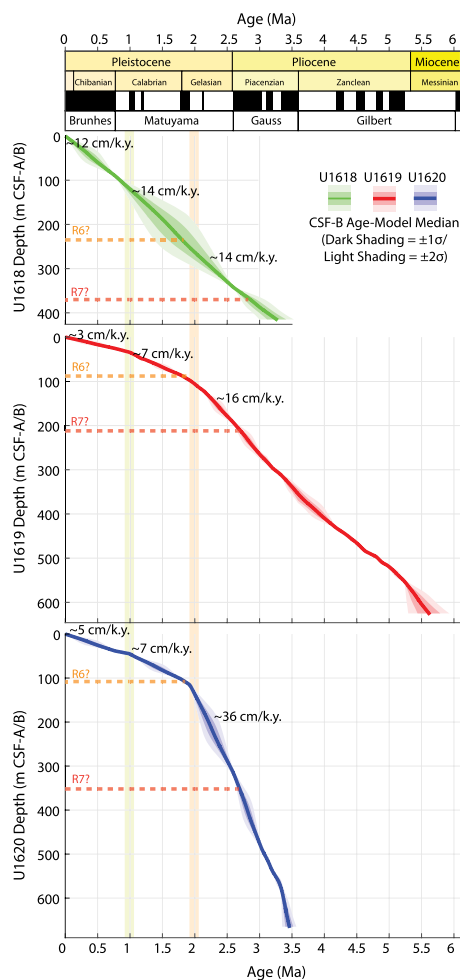


Figure 2. Age models for International Ocean Discovery Program (IODP) Sites U1618 (green), U1619 (red), and U1620 (blue). Time scale is from Gradstein et al. (2020). Depths of R6(?) and R7(?) seismic reflectors are indicated by horizontal dashed lines (see Supplemental Material [text footnote 1]). Core Depth Below Seafloor method A (CSF-A) and method B (CSF-B) are defined in the Supplemental Material.

MATERIALS AND METHODS

Exp403 drilling included two sites in the VR and one site in the SR contourite systems. Site U1618 was drilled into the eastern termination of the VR, which likely overlies continental crust. U1619 lies at the western termination of the VR, and U1620 was drilled into the SR sediment drift (Fig. 1); both overlie oceanic crust. All Exp403 sites are under the influence of the WSC.

Lithostratigraphic intervals were determined through visual description of the split core surfaces, X-radiographs, and smear slides (Lucchi et al., 2026). Age models were constructed using magnetostratigraphic and biostratigraphic data, with uncertainties estimated using the Undatable software (Lougheed and Obrochta, 2019). Long-term average LSRs (cm/k.y.) were determined based on the magnetostratigraphic and biostrati-

graphic age-depth events. See Supplemental Material¹ for coring and age model construction.

RESULTS

Sites U1619 and U1620 extend to the late Miocene and mid-Pliocene, respectively (Lucchi et al., 2026). At both sites, major inflection points in LSRs occur at 2.1–1.8 Ma (base of the Olduvai to the top of the Reunion subchrons; hereafter referred to as ca. 2 Ma) and at ca. 1 Ma (Fig. 2; Table S1). At both of these junctures, LSRs decreased, with the most prominent change at ca. 2 Ma: Site U1620 LSRs decreased from ~36 cm/k.y. to ~7 cm/k.y., and Site U1619 LSRs decreased from ~16 cm/k.y. to ~7 cm/k.y. Circa 1 Ma, LSRs decreased further, to ~5 cm/k.y. at Site U1620 and to ~3 cm/k.y. at Site U1619.

Site U1618 extends to the late Pliocene, slightly older than ca. 2.6 Ma. Here, no change in LSR is observed at ca. 2 Ma, but the ca. 1 Ma inflection point in LSRs is present, marking a decrease in LSRs from ~14 cm/k.y. to ~12 cm/k.y.

The lithostratigraphy at all three sites is primarily siliciclastic, composed of silty clay, clayey silt, clay, and sandy mud (Fig. S2). Major changes in lithology (i.e., divisions of lithologic units or subunits) do not correspond to changes in sedimentation rates. Clast abundance is high since the iNHG, and it is generally higher at Svalbard-proximal Site U1618 with respect to the more distal Sites U1619 and U1620. Laminations are occasionally present, especially in the late Pliocene and older stratigraphic intervals of U1619 and U1620. Bioturbation is more common in all records before ca. 1 Ma (Lucchi et al., 2026). Sediment lithofacies are consistent with deposition by contour currents and ice rafting.

DISCUSSION

Prior to ca. 2 Ma, high LSRs at Site U1620 on the SR were more than double the LSRs for the presumably contiguous VR, to the north. This finding suggests that the SR was a more important depocenter than Johnson et al. (2015) hypothesized, both prior to and continuing through the iNHG. Instead, our results confirm a prediction by Amundsen et al. (2011) of contourite depositional rates as high as 20–40 cm/k.y. on the western flank of the KR. While the iNHG is documented by an increase in clast (dropstone) abundance (Fig. S2), there is no obvious change in LSRs at Site U1619 or Site U1620 (Fig. 2).

The LSRs support the idea that tectonic controls led to differences in accommodation space

available for the depocenter evolution of the VR and SR sediment drifts. However during the past 3.3 m.y., the highest LSR at U1620 reveals that these controls were mainly favorable for sediment deposition south of the MTF (i.e., the SR side; Fig. 3), contrasting the original model of Johnson et al. (2015).

The depositional accommodation space at SR may be the result of significant extensional faulting associated with detachment as the KR opened, followed by subsidence at a highly faulted zone in the corner between the MTF and the KR (Waghorn et al., 2020). This zone was likely subjected to transtensional stresses due to the complex oblique relation between the Molloy and Knipovich spreading ridges (Dumais et al., 2021; Domel et al., 2022). Large-scale basement faults, as well as sedimentary growth faults, are present, including SW of Site U1620 (Fig. S1C). Growth faults reaching close to the present-day seafloor are evidence of movement on previously sedimented detachment faults (Waghorn et al., 2018, 2020). Deposition synchronous with faulting is evidenced by bowed-down seismic reflections at Site U1620 (Fig. S1C). The crustal age and its thermal history, as well as the isostasy effect, are other factors that would influence the amount of accommodation space and deposition regime across the MTF. Such factors require regional investigations, for which these Exp403 findings provide additional motivation.

While tectonic influences such as reduced accommodation space and/or lateral migration of the depocenter away from the main WSC path could contribute to reduced LSRs at SR and VR at ca. 2 Ma, climatic and geomorphic influences on sediment supply to the broader region were also occurring. Decreased LSRs at ca. 2 Ma coincide with the decrease in regional erosion rates as the Eurasian Arctic Barents Shelf switched from subaerial exposure to marine conditions (Patton et al., 2024). A major reduction in sediment supply to the WSC is recorded at the SR and western VR depocenters when the Barents Shelf became marine-based (Fig. 4). No LSR change is recorded at the eastern VR site because of its proximity to Svalbard and thus more continuous influx of glacialic sediments.

A second decrease in LSRs ca. 1 Ma is recorded regionally at all 11 Ocean Drilling Program (ODP) and IODP sites within the WSC influence with sufficient age control or stratigraphic time frame (Fig. 1; Myhre et al., 1995; Channell et al., 1999; Gruetzner et al., 2022; Lucchi et al., 2026). The decrease in LSRs at ca. 1 Ma occurred during the global MPT, a time when glacial cycles transitioned from a dominant low-amplitude 41 k.y. periodicity to a higher-amplitude 100 k.y. dominant periodicity, resulting in more intensified and prolonged glacial periods (Herbert, 2023). The decrease in bioturbation after ca. 1 Ma at the VR and SR

¹Supplemental Material. Further information on Sites U1618, U1619, and U1620 drilling and core recoveries, age models, seismic reflectors, lithostratigraphies, and the tectonic model. Please visit <https://doi.org/10.1130/G54231.1/7813879/g54231.pdf> to access the supplemental material; contact editing@geosociety.org with any questions.

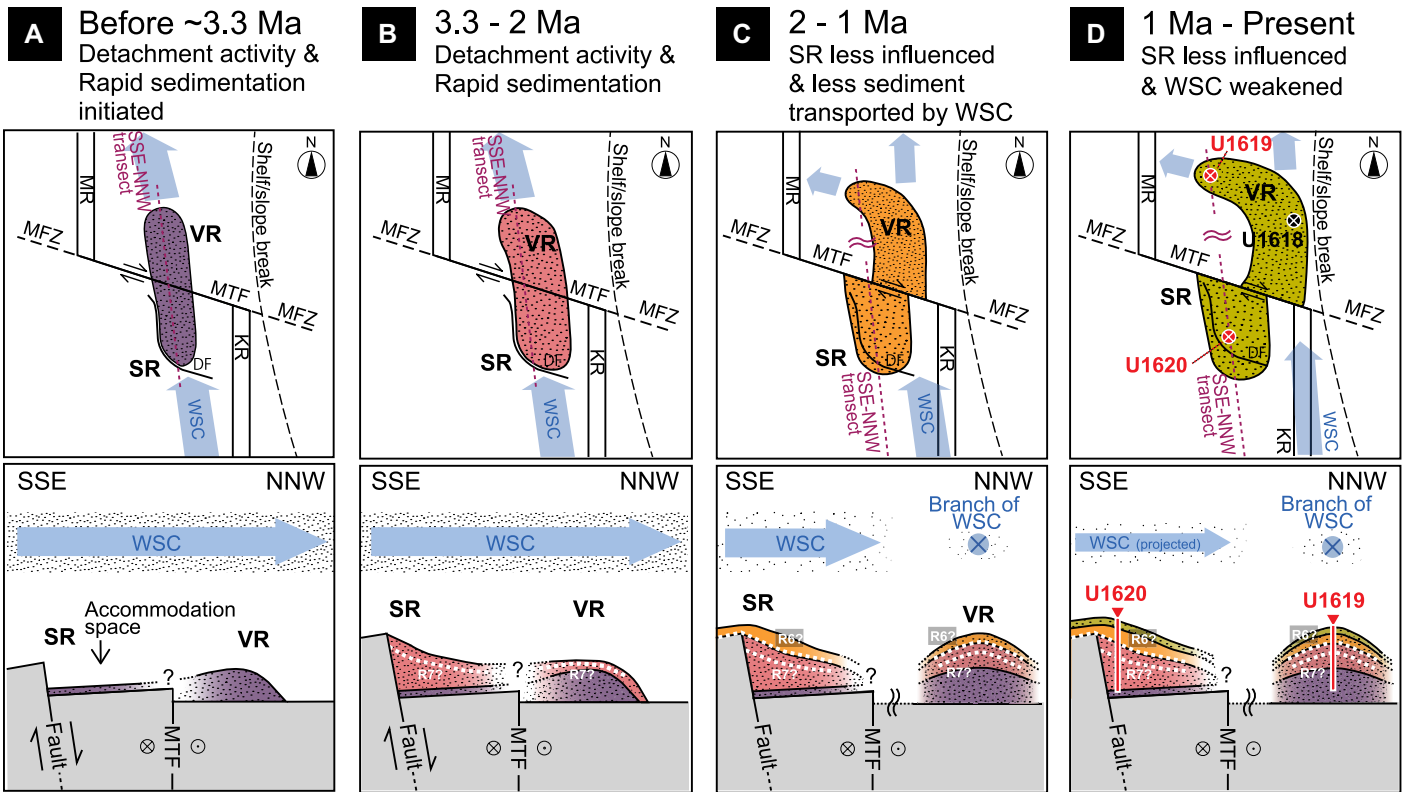


Figure 3. Tectonic influences on sedimentation at Svyatogor Ridge (SR; U1620) and Vestnesa Ridge (VR; U1618 and U1619) sediment drifts through time (A–D) in map and cross-sectional view, after Johnson et al. (2015). Detachment morphology is from Waghorn et al. (2020). Sediment colors represent their relative age. White dashed lines represent seismic reflectors R6(?) and R7(?). See Figure S1 and Table S2 for seismic profiles and reflector data (see text footnote 1). Unknown sedimentary structures were omitted by gradual degrading, denoted with question mark. MR—Molloy Ridge; KR—Knipovich Ridge; MTF—Molloy Transform Fault; MFZ—Molloy Fracture Zone; WSC—West Spitsbergen Current; DF—detachment fault. Dot clouds associated with WSC represent relative volume of sediment transport. W-to-E cross section is shown in Figure S3 (see text footnote 1).

sites may point to less favorable bottom water conditions for benthic life. Changes in ocean circulation and removal of regolith have been proposed as potential triggers for the MPT (Clark and Pollard, 1998; Williams et al., 2024). Nordic coring and climate model simulations suggest that increased Atlantic water inflow to the Arctic Ocean at this time could have accelerated ice-

sheet growth by enhancing precipitation over moderately sized ice sheets (Barker et al., 2021).

Enhanced preferential erosion from more dynamic marine-based ice sheets after 1 Ma in the Barents Shelf region resulted in an intermittently open Barents Seaway when ice free (Patton et al., 2024). By ca. 0.7 Ma, this seaway was permanently in place as an additional circulation

pathway at least during warm times. While long-term average LSRs are not available at a scale to resolve glacials versus interglacials, we propose that the overall decrease in LSRs after ca. 1 Ma observed at the SR, VR, and other sites along the WSC path may be the record of this change in ocean circulation. In sum, after ca. 1 Ma, the WSC weakened and no longer served as the only route for current flow and sediment transport from the North Atlantic to the Arctic (Fig. 4).

If the decrease in LSRs at ca. 1 Ma at sites within the eastern FS reflects a weakening of the WSC, as we propose, then this contrasts with the hypothesis (Barker et al., 2021) of increased Atlantic water inflow to the Arctic based on modeling results and drilling sites in the North Atlantic and Nordic Sea (south of 70°N), and to increased LSRs in the Norwegian Current at this time (Wolf and Thiede, 1991). Reconciliation of these findings with the drilling records from the WSC region is needed. It may be that such reconciliation can be achieved by considering the combined inflow to the Arctic by both the WSC and the Barents Seaway during the MPT.

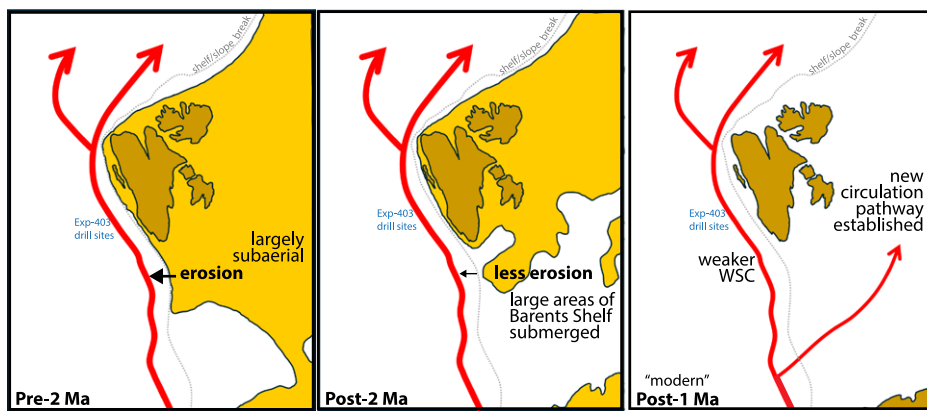


Figure 4. Impact of submergence (at ca. 2 Ma) of Barents Shelf and opening of Barents Seaway (after ca. 1 Ma) on West Spitsbergen Current sediment supply and strength. Current (red arrows), Svalbard (brown), and changing Barents Sea land areas (yellow) are shown. Changes in land area are after Patton et al. (2024).

CONCLUSIONS

Shipboard age models and derived LSRs from IODP Exp403 provide ground-truth data

with which to evaluate previous hypotheses of sediment supply, ice-sheet dynamics, and depocenter evolution at the VR and SR since ca. 3 Ma. Results suggest that the first-order controls on sedimentation rates were a combination of (1) local tectonic-related bathymetric influences on the depocenters, and (2) climate-related regional “up-current” geomorphic influences on erosion rates and paleocurrent patterns affecting sediment supply.

ACKNOWLEDGMENTS

Special thanks go to the International Ocean Discovery Program Expedition 403 (Exp403) project proponents, technicians, and crew. We are grateful for the feedback from P.T. Osmundsen and an anonymous reviewer. Funding for Exp403 and the *JOIDES Resolution* Science Operator (JRSO) was provided via National Science Foundation award OCE1326927. We acknowledge open access funding from MUR for ECORD-IODP Italia and the Geology and Environmental Science Department at James Madison University.

REFERENCES CITED

- Amundsen, I.M.H., Blinova, M., Hjelstuen, B.O., Mjelde, R., and Hafliðason, H., 2011, The Cenozoic western Svalbard margin: Sediment geometry and sedimentary processes in an area of ultraslow oceanic spreading: *Marine Geophysical Researches*, v. 32, no. 4, p. 441–453, <https://doi.org/10.1007/s11001-011-9127-z>.
- Barker, S., Zhang, X., Jonkers, L., Lordsmith, S., Conn, S., and Knorr, G., 2021, Strengthening Atlantic inflow across the mid-Pleistocene transition: Paleooceanography and Paleoclimatology, v. 36, <https://doi.org/10.1029/2020PA004200>.
- Butt, F.A., Drange, H., Elverhøi, A., Otterå, O.H., and Solheim, A., 2002, Modelling late Cenozoic isostatic elevation changes in the Barents Sea and their implications for oceanic and climatic regimes: Preliminary results: *Quaternary Science Reviews*, v. 21, p. 1643–1660, [https://doi.org/10.1016/S0277-3791\(02\)00018-5](https://doi.org/10.1016/S0277-3791(02)00018-5).
- Channell, J.E.T., Smelror, M., Jansen, E., Higgins, S.M., Lehman, B., Eidvin, T., and Solheim, A., 1999, Age models for glacial fan deposits off East Greenland and Svalbard (Sites 986 and 987), in Raymo, M.E., Jansen, E., Blum, P., and Herbert, T.D., eds., *Proceedings of the Ocean Drilling Program, Scientific Results Volume 162: Ocean Drilling Program*, College Station, Texas, http://www-odp.tamu.edu/publications/162_SR/chap_10/chap_10.htm.
- Clark, P.U., and Pollard, D., 1998, Origin of the middle Pleistocene transition by ice sheet erosion of regolith: *Paleooceanography*, v. 13, p. 1–9, <https://doi.org/10.1029/97PA02660>.
- Domel, P., Singhroha, S., Plaza-Faverola, A., Schindwein, V., Ramachandran, H., and Büinz, S., 2022, Origin and periodic behavior of short duration signals recorded by seismometers at Vestnesa Ridge, an active seepage site on the west-Svalbard continental margin: *Frontiers of Earth Science*, v. 10, <https://doi.org/10.3389/feart.2022.831526>.
- Dumais, M.-A., Gernigon, L., Olesen, O., Johansen, S.E., and Brønner, M., 2021, New interpretation of the spreading evolution of the Knipovich Ridge derived from aeromagnetic data: *Geophysical Journal International*, v. 224, p. 1422–1428, <https://doi.org/10.1093/gji/ggaa527>.
- Eiken, O., and Hinz, K., 1993, Contourites in the Fram Strait: *Sedimentary Geology*, v. 82, no. 1–4, p. 15–32, [https://doi.org/10.1016/0037-0738\(93\)90110-Q](https://doi.org/10.1016/0037-0738(93)90110-Q).
- Gaina, C., 2014, Age of Ocean Crust [Dataset]: Geological Survey of Denmark and Greenland (GEUS) Dataverse V1, <https://doi.org/10.22008/UK2/KK5RQN>.
- Gradstein, F.M., Ogg, J., Schmitz, M., and Ogg, G., eds., 2020, *Geologic Time Scale 2020*: Elsevier, 1357 p., <https://doi.org/10.1016/C2020-1-02369-3>.
- Gruetznier, J., Matthiessen, J., Geissler, W.H., Gebhardt, A.C., and Schreck, M., 2022, A revised core-seismic integration in the Molloy Basin (ODP Site 909): Implications for the history of ice rafting and ocean circulation in the Atlantic-Arctic gateway: *Global and Planetary Change*, v. 215, <https://doi.org/10.1016/j.gloplacha.2022.103876>.
- Herbert, T.D., 2023, The mid-Pleistocene climate transition: *Annual Review of Earth and Planetary Sciences*, v. 51, p. 389–418, <https://doi.org/10.1146/annurev-earth-032320-104209>.
- Johnson, J.E., Mienert, J., Plaza-Faverola, A., Vadakkepuliambatta, S., Knies, J., Büinz, S., Andreasse, K., and Ferré, B., 2015, Abiotic methane from ultraslow-spreading ridges can charge Arctic gas hydrates: *Geology*, v. 43, no. 5, p. 371–374, <https://doi.org/10.1130/G36440.1>.
- Kalhagen, K., Skogseth, R., Baumann, T.M., Falck, E., and Fer, I., 2024, An emerging pathway of Atlantic water to the Barents Sea through the Svalbard Archipelago: Drivers and variability: *Ocean Science*, v. 20, p. 981–1001, <https://doi.org/10.5194/os-20-981-2024>.
- Kremer, A., Stein, R., Fahl, K., Ji, Z., Yang, Z., Wiers, S., Matthiessen, J., Forwick, M., Löwemark, L., O’Regan, M., Chen, J., and Snowball, I., 2018, Changes in sea ice cover and ice sheet extent at the Yermak Plateau during the last 160 ka—Reconstructions from biomarker records: *Quaternary Science Reviews*, v. 182, p. 93–108, <https://doi.org/10.1016/j.quascirev.2017.12.016>.
- Lougheed, B.C., and Obrochta, S.P., 2019, A rapid, deterministic age-depth modeling routine for geological sequences with inherent depth uncertainty: *Paleoceanography and Paleoclimatology*, v. 34, no. 1, p. 122–133, <https://doi.org/10.1029/2018PA003457>.
- Lucchi, R.G., St. John, K., Ronge, T.A., and the Expedition 403 Scientists, 2026, *Proceedings of the International Ocean Discovery Program, Volume 403*: College Station, Texas, International Ocean Discovery Program, 426 p., <https://doi.org/10.14379/iodp.proc.403.2026>.
- Myhre, A.M., et al., 1995, *Proceedings of the Ocean Drilling Program, Initial Reports Volume 151*: College Station, Texas, Ocean Drilling Program, 403 p., <https://doi.org/10.2973/odp.proc.ir.151.1995>.
- Patton, H., Alexandropoulou, N., Lasabuda, A.P.E., Knies, J., Andreassen, K., Winsborrow, M., Sverre Laberg, J., and Hubbard, A., 2024, Glacial erosion and Quaternary landscape development of the Eurasian Arctic: *Earth-Science Reviews*, v. 258, <https://doi.org/10.1016/j.earscirev.2024.104936>.
- Rebesco, M., Hernández-Molina, F.J., Van Rooij, D., and Wählin, A., 2014, Contourites and associated sediments controlled by deep-water circulation processes: State-of-the-art and future considerations: *Marine Geology*, v. 352, p. 111–154, <https://doi.org/10.1016/j.margeo.2014.03.011>.
- Waghorn, K.A., Büinz, S., Plaza-Faverola, A., and Johnson, J.E., 2018, 3D seismic investigation of a gas hydrate and fluid flow system on an active mid-ocean ridge: Svyatogor Ridge, Fram Strait: *Geochemistry, Geophysics, Geosystems*, v. 19, p. 2325–2341, <https://doi.org/10.1029/2018GC007482>.
- Waghorn, K.A., Vadakkepuliambatta, S., Plaza-Faverola, A., Johnson, J.E., Büinz, S., and Waage, M., 2020, Crustal processes sustain Arctic abiotic gas hydrate and fluid flow systems: *Scientific Reports*, v. 10, 10679, <https://doi.org/10.1038/s41598-020-67426-3>.
- Walczowski, W., and Piechura, J., 2011, Influence of the West Spitsbergen Current on the local climate: *International Journal of Climatology*, v. 31, no. 7, <https://doi.org/10.1002/joc.2338>.
- Williams, T.J., Piotrowski, A.M., Howe, J.N.W., Hillenbrand, C.-D., Allen, C.S., and Clegg, J.A., 2024, The role of ocean circulation and regolith removal in triggering the mid-Pleistocene transition: Insights from authigenic Nd isotopes: *Quaternary Science Reviews*, v. 345, <https://doi.org/10.1016/j.quascirev.2024.109055>.
- Wolf and Thiede, 1991, History of terrigenous sedimentation during the past 10 m.y. in the North Atlantic (ODP Legs 104 and 105 and DSDP Leg 81): *Marine Geology*, v. 101, p. 83–102, [https://doi.org/10.1016/0025-3227\(91\)90064-B](https://doi.org/10.1016/0025-3227(91)90064-B).
- Zieba, K.J., Omosanya, K.O., and Knies, J., 2017, A flexural isostasy model for the Pleistocene evolution of the Barents Sea bathymetry: *Norsk Geologisk Tidsskrift*, v. 97, no. 1, p. 1–19, <https://doi.org/10.17850/njg97-1-01>.

Printed in the USA